Stark broadening of the hydrogen resonance line L_β in a dense equilibrium plasma

K. Grützmacher and B. Wende
Physikalisch-Technische Bundesanstalt, Institut Berlin, Abbestrasse 2-12, D-1000 Berlin 10, Germany
(Received 22 May 1978)

Profiles of L_β emitted from small hydrogen additions in a dense argon plasma ($n_e = 1$, 2, and 3×10^{23} m^{-3}, $T \approx 10^4$ K) were measured under controlled optical depth over wavelength separation $\Delta\lambda$ from $\lambda_{L\beta}$ of about eight times the half-halfwidth $\Delta\lambda_{1/2}$. Reabsorption in the boundary layers of the plasma, usually caused by hydrogen as well as argon atoms, was avoided. The Stark profiles $P(\Delta\lambda)$ obtained (uncertainty $\pm 4\%$ for $|\Delta\lambda|/\Delta\lambda_{1/2} \leq 4$) were found to be for $|\Delta\lambda|/\Delta\lambda_{1/2} > 0.6$ in good agreement with calculations according to the "unified" theories (Vidal *et al.* and Seidel) and to the modified impact theories (Griem and Bacon). For $|\Delta\lambda|/\Delta\lambda_{1/2} < 0.6$ deviations remain, particularly in the line center, even when time ordering and ion dynamics (Seidel) are taken into account. These residual discrepancies indicate, in accordance with deviations recently found for L_α, that broadening mechanisms which are not finally identified are efficacious. The experimental L_β profiles exhibit an asymmetry behavior similar to that calculated by Bacon, yielding that the asymmetry is mainly caused by ion-field inhomogeneities. Using the scale of angular frequencies the change of sign of the asymmetry is found to be at $\Delta\omega/\Delta\omega_{1/2} = 0.5$, whereas it is predicted by Bacon at $\Delta\omega/\Delta\omega_{1/2} = 1.2$. The measurements indicate red shifts of the centers of the profiles of about $10^{-2}\Delta\omega_{1/2}$ ($\simeq 10^{-3}$ nm for $n_e = 2 \times 10^{23}$ m^{-3}).

I. INTRODUCTION

In the line center, Stark profiles measured for Balmer lines (see, e.g., Ref. 1) emitted from dense plasmas deviate from those calculated according to the modified impact theory (Griem[2]) and the unified theory (Vidal *et al.*[3]). From detailed investigations of the Balmer lines, particularly by varying the reduced masses of the emitter-perturber system (Refs. 4 and 5) it was concluded (Ref. 5) that these discrepancies vanish if ion dynamics and time ordering (Ref. 6) are taken into account for the calculations. Later, large discrepancies were found for L_α (Ref. 7), for which measured halfwidths are larger by a factor of 2.5 than those calculated according to Griem[2] and Vidal *et al.*[3] This could be expected because the Balmer lines compared with the Lyman lines cannot reveal as sensitively the details of the broadening mechanisms owing to the overlapping effects of the numerous Stark components of the upper and lower levels in the case of the Balmer lines. Recent calculations by Seidel,[8] using the model microfield method (Ref. 9), yield that significant deviations remain for L_α even when time ordering and ion dynamics are taken into account. These residual discrepancies indicate that broadening mechanisms are efficacious, which are not finally identified. Theoretical estimates by Griem[10] for L_α, allowing for electron-produced low-frequency fields, yield an additional broadening which may be responsible for the discrepancies observed. For a final interpretation, however, the contribution of this effect has to be studied additionally for other hydrogen lines, in particular for L_β.

From the experimental point of view L_β is more suitable than L_α for an investigation of second-order effects, such as ion-field inhomogeneity and quadratic Stark effect, by measuring the shift and the asymmetry behavior of the profile. The influence of second-order effects was recently studied by Bacon[11] using the impact theory.

In the earliest experiment, Elton and Griem,[12] using a shock tube, showed that their relative intensity measurements of the L_β wings were in agreement with the earlier calculations of Griem *et al.*[13,14] The detailed measurements recently performed by Fussmann,[15] using an argon arc plasma, are particularly falsified by reabsorption in the cooler layers outside of the plasma due to the wing of the argon resonance line.

For our measurements we have chosen an argon arc plasma with small hydrogen additions which was operated at comparatively high number densities of the electrons ($n_e \geq 10^{23}$ m^{-3}). The L_β measurements required the circumvention of the well known reabsorption problem in the cooler boundary layers outside the plasma caused by hydrogen as well as by argon atoms. With increasing n_e some advantages are implied for the investigations: (i) the L_β profiles become nearly true Stark profiles (Doppler and van der Waals broadening become negligible); (ii) the influence of the ion dynamics decreases (this is advantageous for investigations of unidentified contributions to Stark broadening); (iii) the asymmetry caused by second-order effects increases.

The advanced status of the theories necessitates

a detailed comparison of normalized experimental and theoretical profile values instead of a comparison of shape parameters as half widths and dips. For this purpose, the measurements of L_β profile values were extended to wavelength separations $\Delta\lambda$ from λ_{L_β} of about 8 times the half halfwidth $\Delta\lambda_{1/2}$ in order to guarantee that uncertainties due to the required normalization are insignificant.

II. EXPERIMENTAL SET UP, METHODS, AND PLASMA PARAMETER

A. Arc source and spectrometer

The L_β line radiation was excited in a common wall-stabilized cylindrical arc operated in argon with small hydrogen additions [4-mm channel diameter; 80-mm length; current between 40 and 220 A; pressure between 1.1 and 4 bars; concentration of hydrogen (H_2) in argon between less than 2 and 3×10^3 ppm]. The arc plasma was observed in end-on direction at the anode side (1 : 100 beam aperture) and was focused by a platinum-coated mirror (1.4-m focal length) 1.36-fold enlarged onto the entrance slit of a highly resolving Eagle mount spectrometer which was equipped with a MgF_2-coated holographic concave grating (1200 lines per mm; 3-m radius of curvature). For slit widths of 6 μm at the exit and entrance and for an entrance slit height of 100 μm a spectral bandwidth of the spectrometer of 3×10^{-3} nm (full halfwidth of the instrumental function) was found in the region around 120 nm. For the radiation measurement a windowless photomultiplier (EMI, type 9643/2B) was used. In the L_β region the measured relative spectral change of the overall response of the vacuum-uv optical system was about 3% per nm. Wavelength positions of the spectrometer were stable within an uncertainty of 10^{-3} nm during one day and the spectrum could be scanned in steps of 2.8×10^{-4} nm. Counting rates corresponding to measured photomultiplier currents and wavelength positions were fed on line into a Hewlett-Packard data processing system MX 21 which performed the total data evaluation up to the final results as given in Figs. 2–5.

B. Differential pumping system and gas handling

The wall-stabilized arc was connected to the vacuum-uv optical system using a differential pumping system of three stages which allowed a plasma pressure of more than 4 bars in the arc chamber to be reduced less than 10^{-9} bar. In addition, reliable measurements of strong resonance lines excited in a dense plasma require some attention with respect to the connection of the arc source and the differential pumping system (Fig. 1). To avoid reabsorption in cooler boundary layers, the first diaphragm of the pumping system (0.6-mm diam.) was located between the three anodes of the arc close to the end of the plasma column, so that the high-pressure plasma expanded into the pumping system and recombined at pressures which were several orders of magnitude below the pressure in the arc chamber. This operating mode will be called the "reabsorption-free mode" [Fig. 1(a)].

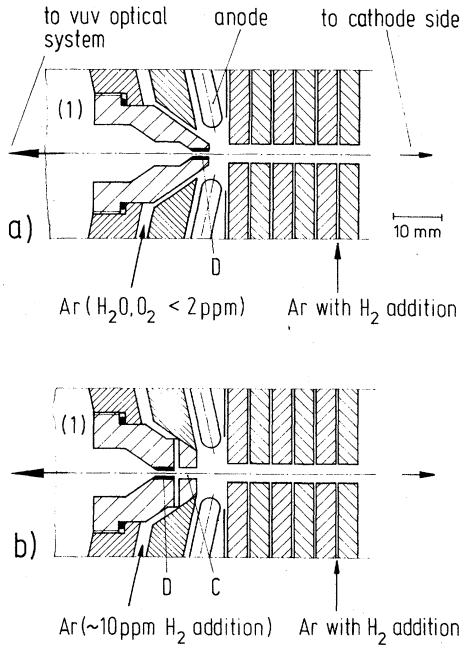

FIG. 1. Arrangement of the diaphragm D between the arc chamber and the chamber (1) of the differential pumping system. (a) Reabsorption-free mode, the plasma expands into the differential pumping system, hence cool boundary layers are avoided. (b) Reabsorption mode, a region of cool argon C (length 5 mm) separates the plasma column from the diaphragm D.

For the measurement of the hydrogen resonance lines the hydrogen concentration had to be kept small in the anode region. This was achieved by a continuous stream of highly purified argon (impurities of H_2O and O_2 less than 2 ppm) which was fed into the arc chamber at the anode side and left the arc channel at the cathode side (typical flow rate 13 $cm^3 s^{-1}$). In particular, O_2 impurities have to be small in order to obtain L_β profiles free of distorting O I lines. The hydrogen was fed into the arc channel at a distance of 22 mm from the anode side of the plasma column using a gas mixture of argon and hydrogen having hydrogen concentrations between 10^2 and 5×10^4 ppm.

In this way a constant hydrogen concentration in the arc column axis was reached within 10 min and hydrogen concentrations (H_2) between 10 and 3×10^3 ppm could be obtained with a relative change of less than 2% during a time interval of more than 1 h which was sufficient for several runs of L_β profile measurements.

The described system [Fig. 1(a)] allows observation of the hydrogen resonance lines without reabsorption in the boundary layers caused by hydrogen atoms themselves (see the measurements of L_α in Ref. 7). In the case of L_β the vicinity of the Ar I resonance line ($\lambda_{ArI} = 104.822$ mn, $\lambda_{L_\beta} = 102.572$ nm) leads to further reabsorption due to the argon atoms which can strongly distort the L_β profile. In this experiment the profile measurements are not falsified due to the argon reabsorption up to $\lambda - \lambda_{L_\beta} = 1$ nm. In order to characterize the efficiency of the system in the reabsorption-free mode, it may be mentioned that the half halfwidth of the reabsorption dip within the argon resonance line is only 0.1 nm for a plasma pressure of 1.1 bar.

A careful determination of the wavelength position $\Delta\lambda = 0$ (corresponding to the wavelength λ_{L_β}) is required for all statements concerning the line shift and the asymmetry behavior of the L_β profile. For this purpose L_β profiles with sharp L_β reabsorption dips (half halfwidths $<4\times10^{-3}$ nm) were generated by using a modified version of the differential pumping system. In the "reabsorption mode" [Fig. 1(b)] the first diaphragm of the differential pumping system was separated from the plasma column by a region of cool argon (5-mm length) with hydrogen additions on the order of 10 ppm.

C. Choice of plasma parameters

The L_β measurements were performed at electron densities $n_e = (1, 2, \text{and } 3)\times10^{23}$ m^{-3} generated at plasma pressures of 1.1 and 2 bars. High values of n_e were chosen, because the interesting asymmetry of L_β could be expected to increase with n_e and the influence of Doppler broadening on the profiles becomes negligible. Values of $n_e < 10^{23}$ m^{-3} were not used because in this case deviations from the local thermodynamic equilibrium (LTE) model may occur causing some complications for the evaluation of the measurements to arise. Although the arc source enabled us to provide electron densities of more than 3×10^{23} m^{-3} at higher plasma pressures it seemed unreasonable to us to measure L_β at these parameters, because the argon background intensity determined by the wing of the Ar I resonance line increases to more than 75% of the source function at $\Delta\lambda = -1$ nm ($n_e = 4\times10^{23}$ m^{-3}; $p = 4$ bars; $\Delta\lambda$ is defined in Ref. 16). In the chosen range of $n_e = (1-3)\times10^{23}$ m^{-3} the corresponding argon background intensity is sufficiently small and varies between 4.5% and 14% of the source function at $\Delta\lambda = +1$ nm and between 9% and 36% at $\Delta\lambda = -1$ nm.

D. Plasma diagnostics

The comparison of measured and calculated L_β Stark profiles necessitates an accurate determination of the number density of the electrons n_e and an approximate determination of the temperature T. Number densities n_e were determined with an uncertainty $\Delta n_e/n_e < \pm 0.1$ by measuring the continuous radiation at $\lambda = 481.6$ nm and by applying a ζ factor of 2.0 ± 0.1 as measured in Ref. 17. The LTE model is sufficiently approximated for an argon arc plasma of the given electron number density $n_e \geq 10^{23}$ m^{-3}. Therefore T was calculated from equilibrium relations from measured values of n_e or was taken as given in Ref. 18 (uncertainty $\Delta T/T < 0.03$).

When small hydrogen additions are fed into a pure argon plasma (arc current and pressure constant), T and n_e increase slightly. This behavior was determined from measured changes of the source function of the krypton resonance line at 123.6 nm applying Planck's law and LTE relations. The maximum increase of the source function and the corresponding increase of n_e (1.1% for the source function, 0.7% for n_e) occurs at the lowest electron density of 1×10^{23} m^{-3} and at H_2 concentrations of 3×10^3 ppm and is negligibly small. The corresponding increase of the argon background is more significant and was therefore taken into account in the evaluation procedure (see Sec. III B).

III. MEASUREMENT AND EVALUATION

A. Procedure of the line-profile measurement

The measurements for determining the L_β profile function P^{exp} [normalization see Eq. (4)] were extended to wavelength separations $|\Delta\lambda| = 1$ nm (about 8 times the half halfwidth) so that 98% of the total line absorption coefficient were obtained. In order to determine the L_β profile function in this region, it was necessary to measure the central region, the near wings, and the wings successively, using stepwise increasing hydrogen concentrations of the arc plasma. The different types of measurements are symbolized by the integers $j = 1, 2, \ldots, 6$ in Table I. For $j = 2, \ldots, 6$ the optical depth of the plasma $\tau(\lambda)$ was set in the recorded wavelength interval $\Delta\lambda_r$ to different maximum value τ_{max} by adjusting the hydrogen concentration

TABLE I. Set of measurements were performed in order to determine one profile of L_β. For the measurement of the spectral radiances (L_λ^{Ar+H}, S_λ) the optical depth of the plasma was set in the recorded wavelength interval $\Delta\lambda_r$ to different maximum values τ_{max}. The set of data was measured for $n_e = 1\times10^{23}$ m^{-3} at a plasma pressure p = 1.1 bar, for $n_e = 2\times10^{23}$ m^{-3} at p = 1.1 and 2 bars, for $n_e = 3\times10^{23}$ m^{-3} at p = 2 bars.

j	Type of measurement	Spectral[a] radiance	Wavelength interval $\Delta\lambda_r$ (nm)	τ_{max}	Number of records
1	argon background	L_λ^{Ar}	±1.0	0.09–0.45[b]	10
2	L_β central region	L_λ^{Ar+H}	±0.17	0.4	10
3	L_β central region with reabsorption dip[c]		±0.17	0.4	10
4	L_β near wing		±0.33	1	10
5	L_β wing		±1.0	2.5	6
6	L_β wing and source function	S_λ	±1.0	$\gg 1$	4

[a] The corresponding photomultiplier currents are $i^{Ar}(\Delta\lambda)$, $i^{Ar+H}(\Delta\lambda)$, and $i^S(\Delta\lambda)$.

[b] τ_{max} of the argon background at $\Delta\lambda = -1$ nm (red side of the L_β profile) depends strongly on the plasma parameters.

[c] For these measurements the differential pumping system was used in the "reabsorption mode" [Fig. 1 (b)].

to the required level between 200 and 3×10^3 ppm. The optical depth $\tau(\lambda)$ was determined according to Eq. (1),

$$\tau(\lambda) = -\ln(1 - L_\lambda^{Ar+H}/S_\lambda) \ . \qquad (1)$$

S_λ is the measured source function (j = 6, Table I) and L_λ^{Ar+H} the spectral radiance of the plasma determined by the argon background intensity and the L_β intensity. As a first step of data reduction, the measurements (see column 6 in Table I) were averaged for each integer j and the measured time-dependent change of the spectral response of the vacuum-uv optical system was taken into account. This change was smaller than 2% for an operating time of 1 h.

B. Radiative transfer

From equations of radiative transfer applied to an argon plasma column containing hydrogen additions in a region of the length L_H the expression

$$\kappa(\Delta\lambda) = \frac{1}{L_H}\ln\left(\frac{S_\lambda - L_\lambda^{Ar}}{S_\lambda - L_\lambda^{Ar+H}}\right) \qquad (2)$$

can be obtained for the absorption coefficient $\kappa(\Delta\lambda)$ of L_β. L_λ^{Ar+H} is the spectral radiance emitted from the plasma column, whereas L_λ^{Ar} would be the emitted spectral radiance if the hydrogen emission did not contribute to the radiation of the plasma column. Variations of the source functions S_λ owing to the small hydrogen concentrations have to be negligibly small (as realized in the experiment, see Sec. II D). If the spectral radiances S_λ, L_λ^{Ar} and L_λ^{Ar+H} are substituted by the corresponding photomultiplier currents i one obtains

$$\kappa(\Delta\lambda) = \frac{1}{L_H}\ln\left(\frac{i^S(\Delta\lambda) - i^{Ar}(\Delta\lambda)}{i^S(\Delta\lambda) - i^{Ar+H}(\Delta\lambda)}\right) \ . \qquad (3)$$

This expression was applied in order to calculate (Ref. 19) $\kappa(\Delta\lambda)$ values of L_β from the sets of measurements listed in Table I.

$\kappa(\Delta\lambda)$ can be determined without knowing the overall spectral response of the vuv optical system. In addition, reabsorption of the radiation in the boundary layers of the plasma does not falsify the determination of $\kappa(\Delta\lambda)$ according to Eq. (3) if all quantities S_λ, L_λ^{Ar}, and L_λ^{Ar+H} underlie identical reabsorption. In general the generation of the source function S_λ is limited to wavelength separations of a few halfwidths of the optical thin line. Therefore one is forced to extrapolate measured $i^S(\Delta\lambda)$ to larger wavelength separations. In the case of strong wavelength-dependent reabsorption (e.g., due to the wing of the argon resonance line) this extrapolation may lead to significant errors (having, e.g., falsified Fussmann's L_β wing results, see Sec. IV C). For the determination of the relative wavelength dependence of $i^S(\Delta\lambda)$ the source function was generated in this experiment for wavelength separations $|\Delta\lambda| \leq 0.2$–0.3 nm (H_2 concentrations about 3%). Then measured $i^S(\Delta\lambda)$ were linearly extrapolated to larger values

of $|\Delta\lambda|$ which is justified because the reabsorption due to the wing of the argon resonance line was negligible (see Sec. II B).

Finally it may be mentioned that L_λ^{Ar} is approximately equal to the spectral radiance of the pure argon plasma ($j = 1$, Table I). The slight increase of L_λ^{Ar} caused by the hydrogen additions was measured at $\lambda = 110.5$ nm (red wings of the argon resonance lines, well separated from L_α and L_β) and was taken into account for the evaluation in Eq. (3). The observed maximum increase of L_λ^{Ar} was found to be 2.5%, occurring for the lowest electron density 1×10^{23} m^{-3} at H_2 concentrations of 3×10^3 ppm.

C. Other broadening mechanisms

The L_β profiles [$\kappa(\Delta\lambda)$, Eq. (3)] obtained for the central region ($|\Delta\lambda| \leq 0.17$ nm) are weakly influenced by Doppler broadening. A proper comparison with calculated Stark profiles therefore requires a deconvolution with respect to Doppler broadening.

This was performed by applying Fourier analysis reducing the problem of solving the integral equation to the calculation of the ratios of Fourier coefficients. The maximum corrections of $\kappa(\Delta\lambda)$ owing to the deconvolution procedure were found to be about 2%.

In order to investigate the influence of van der Waals broadening due to the argon atoms, L_β profiles were compared for $n_e = 2\times10^{23}$ m^{-3} generated at plasma pressures of 1.1 and 2 bars, corresponding to a variation of the number density of the argon atoms by a factor of 10 (calculated from LTE relations). Because of the good agreement [see Table II, footnote (a)], we conclude that van der Waals broadening is insignificant. This could

TABLE II. Comparison of theoretical and experimental L_β profiles for three values n_e. In order to simplify the comparison of symmetric profiles (calculated by Griem,[2] Vidal *et al.*,[3] and Seidel[23]) and slightly asymmetric ones (measured in this work and calculated by Bacon[11]) mean values $P = \frac{1}{2}(P_{red} + P_{blue})$ were used for the calculation of deviations. The deviations, $100(P^{theor} - P^{exp})/P^{exp}$, of the calculated profile values from measured ones are given. Additionally, the measured values P_{red}^{exp} and P_{blue}^{exp} with the corresponding uncertainties are listed. $\Delta\lambda$ is the wavelength separation from λ_{L_β} (Ref. 16) and $\Delta\lambda_{1/2}$ the measured half halfwidth; $\alpha = \Delta\lambda/(1.25\times10^{-14} n_e^{2/3})$ with $\Delta\lambda$ in nm and n_e in m^{-3}. Electron densities and corresponding temperatures (uncertainties: $\Delta n_e/n_e < \pm0.10$; $\Delta T/T < \pm0.03$) are as follows: $n_e = 1\times10^{23}$ m^{-3} at $T = 12\,700$ K; $n_e = 2\times10^{23}$ m^{-3} at $T = 16\,000$ K and $T = 13\,300$ K[a]; $n_e = 3\times10^{23}$ m^{-3} at $T = 14\,800$ K.

		Deviations in %							
	n_e	Unified theories		Modified impact theories		$P^{meas}(\Delta\lambda)$			
$\lvert\Delta\lambda\rvert/\Delta\lambda_{1/2}$	(10^{23} m^{-3})	Vidal *et al.*	Seidel	Griem	Bacon	red	blue		$\lvert\Delta\lambda\rvert$ (nm)	$\lvert\alpha\rvert$ (10^{-3})
	1	−29	− 8	−32	−21	128			0.0	0.0
0	2	−28	−11	−32	−20	130			0.0	0.0
	3	−26	−11	−30	−18	134			0.0	0.0
	1	+16		+ 8	+ 8	154	159		0.0244	0.906
0.37[b]	2	+10				156	163		0.0377	0.882
	3	+ 7				158	167		0.0446	0.885
	1	+ 9				137	135		0.0346	1.47
0.6	2	+ 8			[d]	139	137		0.0612	1.43
	3	+ 5	[d]	[d]		141	138	±4%	0.0804	1.44
	1					79.8	76.5		0.066	2.45
1	2	[d]				81.8	77.7		0.102	2.39
	3					83.6	78.8		0.134	2.39
	1					22.7	21.7		0.132	4.90
2	2	− 7[c]			−10[c]	23.6	22.4		0.204	4.77
	3					24.2	22.8		0.268	4.78
	1					4.52	4.30		0.264	9.80
4	2	− 8[c]	− 6[c]			4.68	4.42		0.408	9.54
	3					4.73	4.45		0.536	9.57
	1					1.17	1.11		0.462	17.2
7	2	− 9[c]	−12[c]			1.20	1.13	±8%	0.712	16.7
	3					1.22	1.14		0.938	16.7

[a] For $n_e = 2\times10^{23}$ m^{-3} the values $P^{exp}(\Delta\lambda)$ were measured at $T = 16\,000$ K ($p = 1.1$ bar) and $T = 13\,300$ K ($p = 2$ bars). The $P^{exp}(\Delta\lambda)$ values differed by less than ±3% for $|\Delta\lambda|/\Delta\lambda_{1/2} \leq 4$. The values given in the table correspond to $T = 16\,000$ K.

[b] $\Delta\lambda/\Delta\lambda_{1/2} \approx \pm0.37$ corresponds to the wavelengths of the L_β peaks.

[c] Given are mean values of the deviations obtained for $n_e = 1, 2$, and 3×10^{23} m^{-3}.

[d] In the regions covered by brackets the deviations are not specified because they are less than ±5%.

be expected because theoretical estimations using the method of Ref. 20 yield that van der Waals broadening and furthermore resonance broadening are negligible under the conditions of this experiment.

Konjevic studied the effect of angular deviations of light rays due to refractive index gradients in plasmas. In Ref. 21 he showed that L_α profiles measured end-on from a pure hydrogen arc (2-mm channel diameter) would be significantly falsified (particularly in the central region) due to the influence of the refractivity corresponding to the L_α transition. For the quite different conditions of this experiment estimations according to Konjevic yield that the refractivity corresponding to the transition L_β and the argon resonance lines have insignificant influence on the L_β profiles obtained.

D. Composition of the total L_β profile and consistency of the evaluation procedure

The final L_β profiles were composed from $\kappa(\Delta\lambda)$ values obtained for the line center (after deconvolution), the near wings, and the wings and then were converted to reduced profiles $P^{\exp}(\alpha)$ by applying the normalization

$$\int_{-\alpha_1}^{\alpha_1} P^{\exp}(\alpha)\, d\alpha + 2\int_{\alpha_1}^{\infty} P^{\mathrm{FW}}(\alpha)\, d\alpha = 1 \qquad (4)$$

α is the reduced wavelength separation in Å per cgs field strength as used in the theories (Refs. 2 and 3)

$$\alpha = \Delta\lambda/F_0; \quad F_0 = 1.25\times10^{-14} n_e^{2/3}\ ; \qquad (5)$$

with $\Delta\lambda$ in nm and n_e in m^{-3}. The first integral in Eq. (4) corresponds to the measured region of the profile (α_1 corresponds to $\Delta\lambda = 1$ nm), whereas the second integral ($\alpha \geq \alpha_1$) is a correction quantity taking into account the far wings $P^{\mathrm{FW}}(\alpha)$ which were not measured. For these residual parts of the profiles 2.3 times the values of the asymptotic Holtsmark wing [see Eq. (7) and Fig. 4] were used. The contribution of the second term in Eq. (4) is small ($\simeq 0.02$). Therefore significant uncertainties of $P^{\mathrm{FW}}(\alpha)$ have insignificant influence on the normalized values $P^{\exp}(\alpha)$ obtained.

By comparing the final L_β profiles in a wavelength range $0.05 \leq |\Delta\lambda| \leq 0.17$ nm with those profiles having the reabsorption dip (measurement $j = 3$ in Table I), the wavelength position $\Delta\lambda = 0$ was determined with an uncertainty $\pm 5\times10^{-4}$ nm by setting the minimum of the sharp L_β reabsorption dip (half halfwidth $<4\times10^{-3}$ nm) equal to the L_β wavelength.

In order to check the quality of the total evaluation procedure, particularly determined by Eq. (3), we composed four final L_β profiles from different types of measurements j (Table I) which correspond to different levels of the hydrogen concentration and the optical depth. The measurements $j = 2, 4, 5$; $j = 2, 4, 6$; $j = 4, 5$; and $j = 4, 6$ were used for the composition. The agreement between the four profile functions $P^{\exp}(\Delta\lambda)$ within $\pm 3\%$ for wavelengths up to $|\Delta\lambda|/\Delta\lambda_{1/2} = 4$ and within $\pm 5\%$ up to $|\Delta\lambda|/\Delta\lambda_{1/2} \simeq 8$ demonstrate the reliability of the measurement and of the evaluation even up to an optical depth $\tau = 1$ (Ref. 19).

IV. COMPARISON BETWEEN THEORETICAL AND EXPERIMENTAL L_β STARK PROFILES

A. General remarks

For all electron densities investigated, in general, a good agreement between the measured profiles $P^{\exp}(\Delta\lambda)$ and the calculated ones $P^{\mathrm{theor}}(\Delta\lambda)$ (Ref. 22) according to the "unified" theories (Vidal *et al.*[3]; Seidel,[23] model microfield method: MMM) and to the impact theories (Griem[2] and Bacon[11]) is found.

Because of the advanced status of the theories it seems necessary to compare in detail $P(\Delta\lambda)$ values in order to obtain additional information on those contributions to Stark broadening which are not finally identified. For the Balmer lines, e.g., in early papers "shape parameters" like halfwidth values and dip parameters were usually discussed because these parameters could be measured more easily than $P(\Delta\lambda)$ values. This discussion seems less useful because it may result in misleading conclusions. This becomes clear from a simple example: for L_β the $P(\Delta\lambda)$ values according to Vidal *et al.*[3] and Seidel[23] agree within 2% at wavelength separations near $\Delta\lambda_{1/2}$, whereas the halfwidths of the profiles differ by about 10% because of different peak heights of the profiles at $\Delta\lambda/\Delta\lambda_{1/2} \simeq \pm 0.37$.

In Fig. 2 measured profile values and calculated values according to the unified theories were compared in order to demonstrate representatively the good general agreement between the theories and the experiment. A more detailed comparison is given for all theories and all investigated values of n_e in Table II for a selected number of wavelength separations given in terms of the measured half halfwidth $\Delta\lambda_{1/2}$. The measured $P^{\exp}(\Delta\lambda)$ values are listed for the blue and red side of the profiles, in order to show the slight asymmetry of the profiles. Excellent agreement between calculated and measured data in the near wing range ($0.6 < |\Delta\lambda|/\Delta\lambda_{1/2} < 2$) for all theories can be recognized, whereas slightly increasing deviations occur for the far wings. The most significant deviations

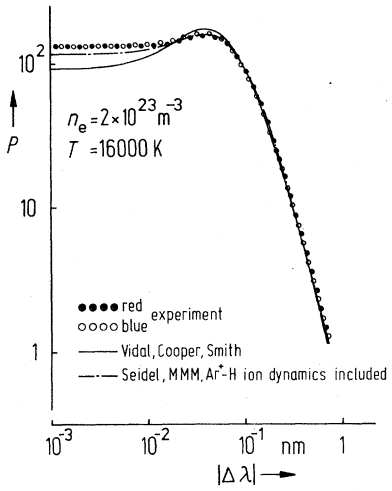

FIG. 2. Measured L_β profile in comparison with "unified" theories.

are found for the central region of the profiles, particularly in the line center. This could be expected, because it is well known that in the central region measurements of the Balmer lines (Ref. 1) and particularly of L_α (Ref. 7) deviate from calculations according to Griem[2] and Vidal *et al.*[3] Our special interest is concentrated, therefore, on this region.

B. Central region

In Fig. 3 calculated L_β profiles are compared with the measured ones for the central region. We have tried to illustrate the different results within the modified impact theories (Griem[2] and Bacon[11]) and within the unified theories (Vidal *et al.*[3] and Seidel[23]). The progress of modified impact calculations, taking into account time ordering and second-order effects (Bacon[11]), can easily be recognized. We see a filling of the central dip (the deviation for $\Delta\lambda = 0$ compared with Griem reduces from −32% to −20%, see Table II) without remarkable influence on the peak heights. The slight asymmetry of the profile according to Bacon (e.g., note the different peak heights) appears due to second-order effects and will be discussed later. The comparison of both the unified theories shows the evident influence of ion dynamics and time ordering simultaneously, because the Seidel calculations include explicitly the ion dynamics while time ordering is implied in the MMM itself. Here the filling of the dip (the deviation reduces from −28% to −11% compared with Vidal *et al.*[3]) appears due to ion dynamics and time ordering, while the lowering of the peaks depends only on the ion dynamics.

Remarkable deviations between experiment and theory remain even for the most advanced calculations of Bacon[11] and Seidel.[23] The residual de-

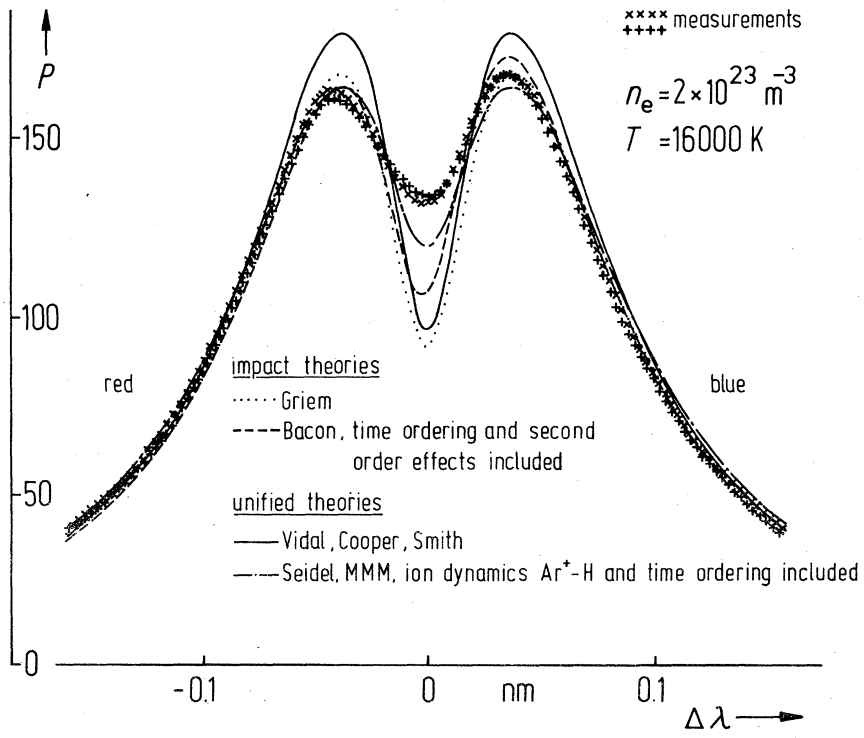

FIG. 3. Central region of measured L_β profiles in comparison with calculated ones in order to demonstrate the predicted contributions to Stark broadening caused by time ordering and ion dynamics. The two measured profiles were obtained under different optical depths ($j = 2$ and 4 in Table I).

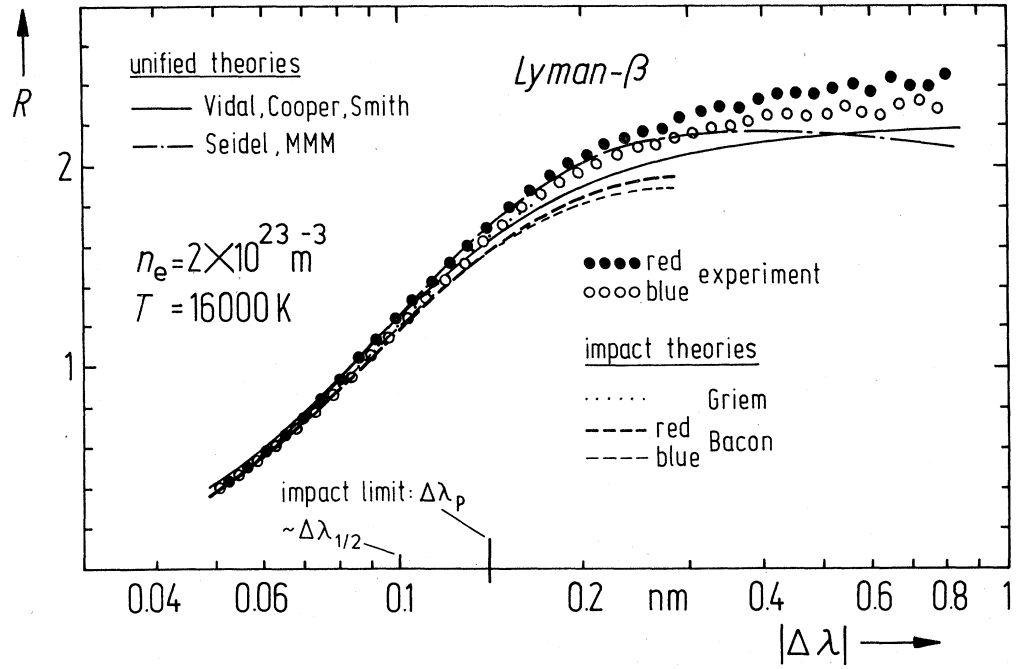

FIG. 4. Measured L_β wings compared with calculated ones using the asymptotic wing representation [Eq. (6)].

viations in the central region indicate that the effects of ion dynamics and time ordering are not the only ones responsible for the deviations in the line center. This is evidently established furthermore by a L_α experiment (Ref. 7). For $n_e = 2 \times 10^{23}$ m^{-3} theoretical Stark profiles deviate in the line center by 22% for MMM results recently calculated by Seidel,[23] +115% for Vidal *et al.*,[3] +93% for Griem,[2] and +60% for Bacon.[11]

From detailed investigations of the Balmer lines (Ref. 5) it was concluded that the disagreement in the central region between theoretical and experimental Stark profiles vanishes, if ion dynamics and time ordering will be taken into account by the theories. Because of the residual discrepancies established by the experimental studies of the Lyman lines, we cannot confirm this conclusion for L_α and L_β.

Theoretical estimates by Griem[10] for L_α allowing for electron-produced low-frequency fields yield an additional broadening which may be responsible for the discrepancies observed. For a final interpretation, however, the contribution of this effect in the case of L_β should be studied.

C. Wings

Theoretical and experimental results of the L_β wings are compared in Fig. 4 applying the asymptotic wing representation R

$$R(\Delta\lambda) = P(\Delta\lambda)/P^H(\Delta\lambda) \ . \tag{6}$$

R is the ratio of profile values P to the corresponding values of the asymptotic Holtsmark wing P^H

$$P^H(\Delta\lambda) = A_{L_\beta} \alpha^{-5/2}(\Delta\lambda, n_e) \tag{7}$$

with $A_{L_\beta} = 1.79 \times 10^{-5}$.

In the wing region of highest experimental accuracy ($|\Delta\lambda|/\Delta\lambda_{1/2} \leq 4$) the best agreement between calculated and measured data is found for Seidel (MMM), whereas the results according to Vidal *et al.* are a few percent smaller (Fig. 4). This may be caused by the contribution of the time-ordering effect implied in the MMM. For $|\Delta\lambda|/\Delta\lambda_{1/2} > 4$ the increasing deviations of the Seidel results may be due to limitations of the computation time (Ref. 23). Deviations found for the Bacon data with increasing $|\Delta\lambda|$ and n_e in the region $|\Delta\lambda|/\Delta\lambda_{1/2} > 2$ can be understood, because this region lies outside of the validity limit of the impact theories (impact limit $\Delta\lambda_p/\Delta\lambda_{1/2} = 1.4$ for $n_e = 2 \times 10^{23}$ m^{-3}; $\Delta\lambda_p$ is the separation corresponding to the plasma frequency ω_p). Although the Griem data show the same tendency with increasing n_e, this is not so obvious, because they are, in general, a few percent higher than the Bacon data (Fig. 4) and were not extended to large values of $|\Delta\lambda|$.

In the earliest experiment, Elton and Griem,[12] using a shock tube ($n_e = 3 \times 10^{23}$ m^{-3}, $T = 20\,000$ K) showed that their relative intensity measurements of the L_β wings were in agreement with the earlier

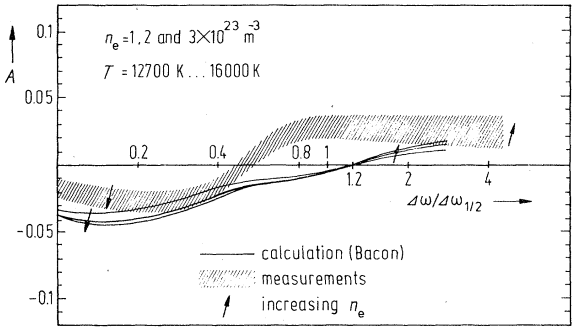

FIG. 5. L_β asymmetry A [Eq. (8)] vs $\Delta\omega/\Delta\omega_{1/2}$ obtained from measured and calculated profiles [$\Delta\omega_{1/2}$ corresponds to measured $\Delta\lambda_{1/2}$]. The shaded region represents about 75% of all asymmetry values obtained.

impact theory of Griem *et al.*[13,14] The reported indication of a L_β blue shift of about 0.02 nm is not confirmed by our measurements which yield a red shift of about 1.5×10^{-3} nm for $n_e = 3\times10^{23}$ m^{-3}.

The measurements recently performed by Fussmann[15] using an arc plasma ($n_e = 0.7\times10^{23}$ m^{-3}, T = 12 200 K) deviate systematically from our results. In the region $0.4 < |\Delta\lambda|/\Delta\lambda_{1/2} < 3$ Fussmann measured about 15% higher profile values for the blue wing than for the red one. This contradiction to our results is mainly caused by two facts. In the region of small values a falsified wavelength reference used by Fussmann is particularly responsible for the discrepancies. The wavelength scale underlying the Fussmann results is based on the value of the unshifted O I line (λ = 102.743 nm) while a red shift had to be considered (about 0.02 nm according to Griem[2]). For larger values $|\Delta\lambda|$ the strong wavelength-dependent reabsorption in Fussmann's experiment due to the wing of the argon resonance line had a systematic falsifying influence on the L_β profile.

D. Shift and asymmetry

Bacon recently studied (Ref. 11) the influence of second-order effects on the broadening of L_α and L_β by treating the quasistatic ion perturbation in a similar manner to that described by Sholin.[24] The predicted asymmetry of these lines is mainly caused by the ion-field inhomogeneity, whereas the quadratic Stark effect is responsible only for a comparatively small contribution. Theoretical L_β profiles according to Griem,[2] Vidal *et al.*,[3] and Seidel[23] are symmetric with respect to the scale of angular frequencies ω. For the dicusssion of the shift and asymmetry of the experimental profiles the use of the scale of angular frequencies seemed adequate to us. It should be mentioned, that the position $\Delta\lambda = 0$ ($\Delta\omega = 0$) in the L_β profiles presented in Table II and Figs. 2–4, corresponds to the wavelength λ_{L_β}, which was determined within an uncertainty of $\pm5\times10^{-4}$ nm using a sharp L_β absorption dip. Computing the centers of the profiles $P^{\exp}(\Delta\omega)$, red shifts of $(1\pm0.5)\times10^{-2}\Delta\omega_{1/2}$ were found (Refs. 25 and 26). For the correct treatment of the asymmetry, it would be necessary to relate the asymmetry to the centers computed. Because of the small red shift and its large uncertainties, it seemed reasonable to us, however, to relate the L_β asymmetry to $\Delta\omega = 0$.

The comparison of the slight asymmetry, seen in calculated L_β profiles (Bacon) and measured ones, requires a sensitive representation. The asymmetry A was calculated using

$$A(\Delta\omega) = \frac{P^{\text{red}}(\Delta\omega) - P^{\text{blue}}(\Delta\omega)}{P^{\text{red}}(\Delta\omega) + P^{\text{blue}}(\Delta\omega)} \quad . \tag{8}$$

If A is presented versus $\Delta\omega/\Delta\omega_{1/2}$ for all investigated values of n_e (Fig. 5), approximately the same result for A is found within comparatively high uncertainties. Asymmetry values, measured and predicted, exhibit the same tendency with both n_e and $\Delta\omega/\Delta\omega_{1/2}$. However, the change of sign (crossover point) comes out at different values $\Delta\omega/\Delta\omega_{1/2}$. For all values n_e investigated, this crossover is found to be at $\Delta\omega/\Delta\omega_{1/2} = 0.5\pm0.05$, whereas it is predicted by Bacon at $\Delta\omega/\Delta\omega_{1/2} = 1.2$.

ACKNOWLEDGMENT

The authors thank U. Johannsen for measuring the change of the plasma parameters caused by small hydrogen additions.

[1] W. L. Wiese, D. E. Kelleher, and D. R. Paquette, Phys. Rev. A 6, 1132 (1972).
[2] H. R. Griem, *Spectral Line Broadening by Plasmas* (Academic, New York, 1974).
[3] C. R. Vidal, J. Cooper, and E. W. Smith, Astrophys. J. Suppl. Ser. 25, 37 (1973).
[4] D. E. Kelleher and W. L. Wiese, Phys. Rev. Lett. 31, 1431 (1973).
[5] W. L. Wiese, D. E. Kelleher, and V. Helbig, Phys. Rev. A 11, 1854 (1975).
[6] L. J. Roszman, Phys. Rev. Lett. 34, 785 (1975).
[7] K. Grützmacher and B. Wende, Phys. Rev. A 16, 243

(1977).
[8]J. Seidel, Z. Naturforsch. A 32, 1207 (1977).
[9]J. Seidel, Z. Naturforsch. A 32, 1195 (1977).
[10]H. R. Griem, Phys. Rev. A 17, 214 (1978).
[11]M. E. Bacon, J. Quant. Spectrosc. Radiat. Transfer 17, 501 (1977).
[12]R. C. Elton and H. R. Griem, Phys. Rev. 135, A1550 (1964).
[13]H. R. Griem, A. C. Kolb, and K. Y. Shen, Phys. Rev. 116, 4 (1959).
[14]H. R. Griem, Astrophys. J. 136, 422 (1962).
[15]G. Fussmann, J. Quant. Spectrosc. Radiat. Transfer 15, 791 (1975).
[16]In order to be compatible with Ref. 11 the wavelength separation $\Delta\lambda$ is defined by $\Delta\lambda = -(\lambda - \lambda_{L\beta})$.
[17]H. Nubbemeyer, J. Quant. Spectrosc. Radiat. Transfer 16, 395 (1976).
[18]H. Nubbemeyer, thesis (Freie Universität Berlin, 1974).
[19]Uncertainties $\Delta\kappa/\kappa$ owing to uncertainties $\Delta S_\lambda / S_\lambda$ increase with the optical depth τ. For optical depths up to $\tau = 1$ uncertainties of $\Delta S_\lambda / S_\lambda = 0.01$ lead to uncertainties $\Delta\kappa/\kappa \simeq 0.02-0.03$ depending on the argon background.
[20]W. R. Hindemarsh and J. M. Farr, *Progress in Quantum Electronics* (Pergamon, Oxford, 1972), Vol. 2, Part 3, pp. 141–214.
[21]N. Konjevic, *Proceedings of Invited Lectures*, VIII. International Summer School on Physics of Ionized Gases, Dubrovnik, 1976.
[22]The L_β profile values $P(\alpha)$ calculated by Vidal, Cooper, and Smith (Ref. 3) are tabulated only up to $n_e = 1 \times 10^{23}$ m^{-3}. The comparison with measured data (n_e up to 3×10^{23} m^{-3}) therefore required an extrapolation which was performed by applying a second-order polynomial method (as suggested for interpolation in Ref. 3). L_β data $P(\alpha)$ according to Griem (Ref. 2), Bacon (Ref. 11), and Seidel (Ref. 23) are tabulated up to $n_e = 10^{24}$ m^{-3} and the interpolations to the desired experimental n_e and T were done using the mentioned method. Equation (5) was used in order to obtain $\Delta\lambda$ values corresponding to the tabulated α values. Although this is commonly accepted, it implies an only approximate transformation from angular frequencies to wavelengths, causing errors with increasing $\Delta\lambda$. The maximum error of the theoretical $P^{\text{theor}}(\Delta\lambda)$ values due to this procedure amounts to $\pm 2\%$ at $\Delta\lambda = \pm 1$ nm (maximum wavelength separation in this experiment).
[23]J. Seidel (private communication).
[24]G. V. Sholin, Opt. Spectrosc. 26, 275 (1969).
[25]For the small range n_e investigated, the measured shift was related to the halfwidth. This does not mean that the shift was found to be proportional to the halfwidth.
[26]$\Delta\omega_{1/2}$ corresponds to measured $\Delta_{1/2}$.